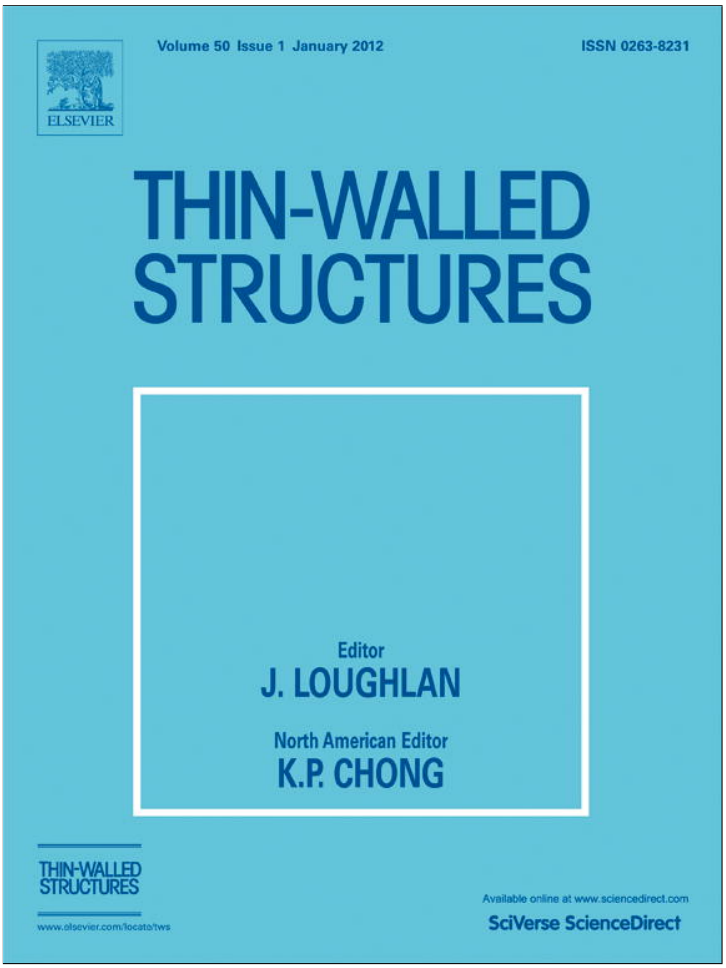

Thin-Walled Structures 68 (2013) 65–74

Contents lists available at SciVerse ScienceDirect

Thin-Walled Structures

journal homepage: www.elsevier.com/locate/tws

Crash analysis and energy absorption characteristics of S-shaped longitudinal members

Ahmed Elmarakbi *, Yee Xin Long, John MacIntyre

Department of Computing, Engineering and Technology, Faculty of Applied Sciences, University of Sunderland, Sunderland, SR6 0DD, UK

ARTICLE INFO

Article history:
Received 26 September 2012
Accepted 5 February 2013

ABSTRACT

This paper presents finite element simulations of the crash behavior and the energy absorption characteristics of thin S-shaped longitudinal members with variable cross-sections made of different materials to investigate the design of optimized energy-absorbing members. Numerical studies are carried out by simulation via the explicit finite element code LS-DYNA [1] to determine the desired variables for the design of energy-absorbing members. The specific energy absorption (SEA), the weight of the members and the peak force responses during the frontal impact are the main measurements of the S-shaped members' performance. Several types of inner stiffening members are also investigated to determine the influence of the additional stiffness on the crash behavior.

1. Introduction

An increasing public awareness of safety issues and stronger legislative requirements have increased the pressure on vehicle manufacturers to improve their vehicles' crashworthiness. The crashworthiness of a vehicle depends on the structure's ability to absorb maximum kinetic energy while maintaining the integrity of the occupant's compartment. In order to ensure the vehicle's structural integrity and its ability to absorb crash energy with minimal diminution of survivable space, it is important to study the crash behavior of the front-end structure to reduce peak forces and improve its energy absorption capacity.

Understanding the crashing behavior of the front-end structure is extremely important because it affects the overall profile of the crash pulse, which is directly related to passenger injury. The frontal safety performance of vehicles is mainly controlled by the collapse behavior of the longitudinal frame members in the front-end structure. Therefore, the longitudinal frame members need to be optimized to perform more progressively and efficiently when accidents happen under any conditions.

There are two main routes to optimize the crash performance of the longitudinal frame member: the introduction of advanced materials with better mechanical properties and geometric optimization of the member (e.g., its wall thickness or cross-section). Analyses of front frame rails including calculations of their energy-absorbing characteristics have been extensively conducted in past decades. Ohkami et al. [2] and Abe et al. [3] carried out experimental and numerical studies on the collapse behavior of S-shaped beams. Reinforcement of the cross-section has been shown to increase the specific energy absorption of the S-shaped longitudinal beam during impact. An experimental study was carried out by Kim and Wierzbicki [4]. In their research, they addressed the design aspect of a front side rail structure of an automobile body and investigated several internal stiffeners to strengthen the longitudinal tubes.

Zhang and Saigal [5] have also studied the effect of different cross-section reinforcement strategies during impacts. They concluded that a structural reinforcement increases the total energy absorption. Tehrani and Nikahd [6,7] investigated different arrangements of straight and oblique ribs on the S-shaped tube in order to control the longitudinal and bending collapses. More recent studies have shown that substitutions with better material are generally more effective than structural modification in improving automobile crashworthiness and in producing lighter weight [7]. Aluminum alloys have been put forward to replace low-strength steel structural components within automobiles. The reason for using these alloys is that the design and manufacturing sectors are now trying to reduce the weight of automobiles while maintaining or improving the energy absorption [8]. Cross-sectional dimensions and material properties are the main considerations used to determine the stiffness, strength and energy absorption of box-type structures. Kim et al. [9] applied loads to hydro-aluminum foam-filled S-shaped tubes. From the deformation pattern of the S-shaped tube, they concluded that ultra-light metallic foam-filling is a good way to strengthen S-frame members. Metallic foam-filler can not only provide the advantage of weight efficiency, but also increases the efficiency of the S-tube due to the contact between the skin and the foam filler. Although this study was positive on the use of the foam-filled S-tube, another study discovered that the addition of aluminum

* Corresponding author. Tel.: +44 1915153877.
E-mail address: ahmed.elmarakbi@sunderland.ac.uk (A. Elmarakbi).

0263-8231/$ - see front matter © 2013 Elsevier Ltd. All rights reserved.
http://dx.doi.org/10.1016/j.tws.2013.02.008

form-filled structures increased the energy absorption but also led to an increase in peak forces. Therefore, the study concluded that even though aluminum foam-fill is an efficient alternative energy absorber, it does not increase the specific energy absorption of the structure due to the increased mass [5]. In addition to aluminum, fiber-reinforced plastic composite materials are also playing a new role in the automotive and aerospace sectors. This material has shown promise in increasing strength, reducing weight and lowering fuel consumption [10]. Finally, Elmarakbi et al. [11] conducted extensive research using finite element simulations of the thin wall tubes in the front-end structure using both material and geometry optimization. They used the optimized members to develop a new vehicle/pole energy absorbing system to enhance vehicle safety.

The aim of this paper is to study the crash behavior and energy absorption characteristics of S-shaped members and to provide shape optimization for better crash responses. A detailed finite element analysis using the explicit code LS-DYNA is carried out using different materials and geometries of the S-shaped frame members. The specific energy absorption (SEA) and the peak crash force are considered in this paper as the main criteria for optimization.

2. Finite element modeling of S-shaped longitudinal members

A model of a thin S-shaped longitudinal member was developed for analysis using the explicit finite element package, LS-DYNA. The S-shaped member has length $L=1000$ mm and a perimeter of 534 mm with different cross-section shapes including a square, rectangle, hexagon and octagon. A schematic diagram of the finite element model with loading and boundary conditions of the axial crush for the two S-shaped front members using an impactor is shown in Fig. 1. Figs. 2 and 3 present a 3-D view of the S-shapes members from the top and side views, respectively.

For quasi-static loading of the tube, other studies have assigned a velocity to move downward until the tube is deformed using the DEFINE_CURVE keyword card. In this paper, it was decided that a more realistic approach would be to assign an initial velocity to the impactor using the initial velocity card followed by the application of a mass to the impactor.

Two material types are used during the simulations. First, a rigid material is applied to the base and impactor using Mat_Rigid (MAT_20). This was done to prevent any deformation of these parts, which could have an undesirable effect on the internal energy and tube deflection results. For the material characteristics of the S-shaped members, MAT_PIECEWISE_LINEAR_PLASTICITY (MAT_24) is assigned to replicate the non-recoverable changes of the tube under applied loads. This study focuses on two types of material, mild steel and aluminum, with mechanical properties as described below [12].

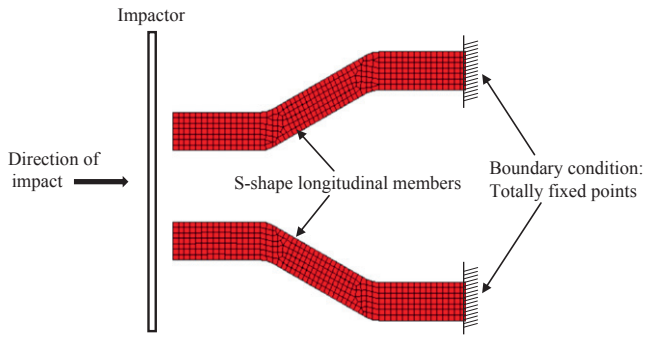

Fig. 1. Finite element modeling with loading and boundary conditions of S-shaped members under impact.

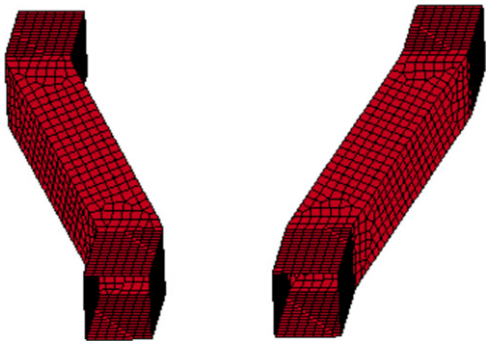

Fig. 2. 3-D view of S-shaped longitudinal members.

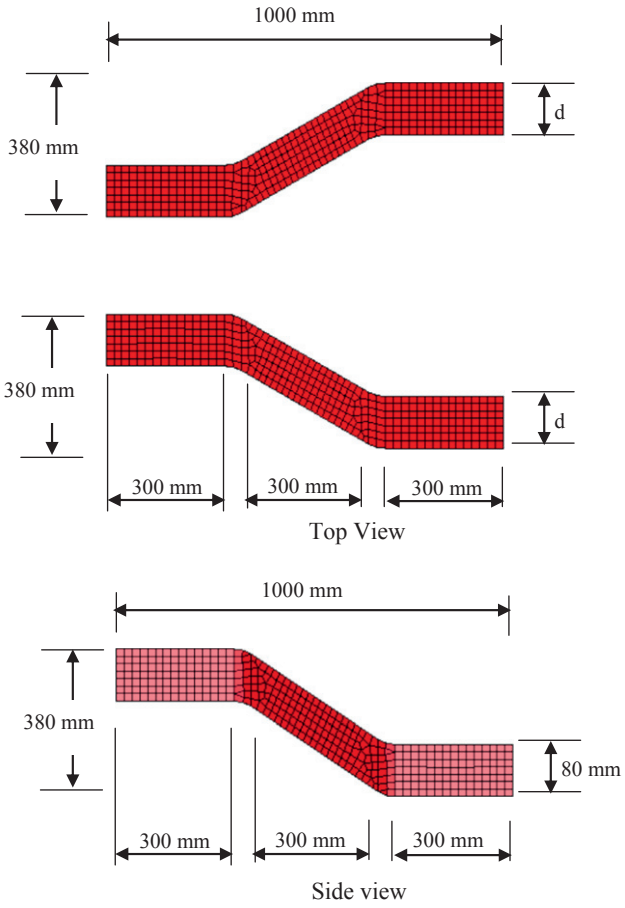

Fig. 3. Configuration of an S-shaped longitudinal member in top and side views.

2.1. Steel

The steel has a density $\rho=7830$ kg/m^3, a modulus of elasticity $E=207$ GPa, a Poisson's ratio $\upsilon=0.28$ and a yield stress $\sigma_y=215$ MPa. The effective plastic strain was taken as 0.0, 0.004, 0.03, 0.15, 0.3 and 0.4 with corresponding stress values of 215, 300, 390, 440, 460, and 400 MPa, respectively.

2.2. Aluminum grade 6063-T5

The aluminum has a density $\rho=27$ kN/m^3, a Young's modulus $E=68.9$ GPa, a yield stress $\sigma_y=145$ MPa and a Poisson's ratio

$\upsilon = 0.33$. The effective plastic strain was taken as 0.0 and 0.08 with corresponding stress values of 145 and 186 MPa, respectively.

To prevent the parts from passing through one another upon impact, several contact cards are assigned to the model. Two contact cards used in each simulation process are the CONTACT_AUTOMATIC_NODES_TO_SURFACE and CONTACT_AUTOMATIC_SINGLE_SURFACE. The automatic nodes-to-surface card is applied for the contact between the members and the impactor. The automatic single surface card is used for the contact between the S-shaped tube members; both the slave and master values are set to 0 as a single surface is assigned for the length of the member. For contact between the tube and impactor, the tube is assigned to be a slave part with the impactor as the master. For the simulation of the axial impact on the S-shaped members, the simulated parts are modeled as shell elements with a fully-integrated shell element formula 16. 5 Gauss integration points through thickness are used to model the shell tube, as progressive plastic folding will occur during the collapse of tubular structures.

3. Numerical simulations

In order to obtain accurate and realistic results, the explicit finite element software LS-DYNA was used to carry out simulations. In this section, the effects of key parameters on the performance of crash behavior and energy dissipation are discussed. These key parameters include impact velocity, cross-sectional shape, material type, thickness and added stiffeners.

Table 1
SEA and peak force of steel and aluminum S-shaped longitudinal members with different cross-sections.

	Aluminum			Steel		
	Weight (kg)	SEA (kJ/kg)	Peak force (kN)	Weight (kg)	SEA (kJ/kg)	Peak force (kN)
Hexagon	4.707	0.873	46.887	13.651	1.052	130.473
Octagon	4.707	0.870	46.057	13.651	1.038	124.289
Rectangle	4.728	0.715	30.894	13.712	0.876	90.565
Square	4.716	0.804	36.061	13.675	0.962	104.450

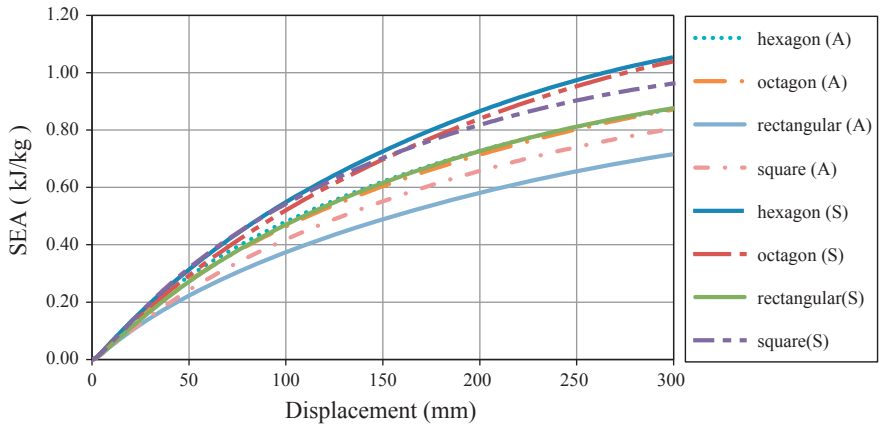

Fig. 4. SEA vs. displacement for steel and aluminum with different cross-sections.

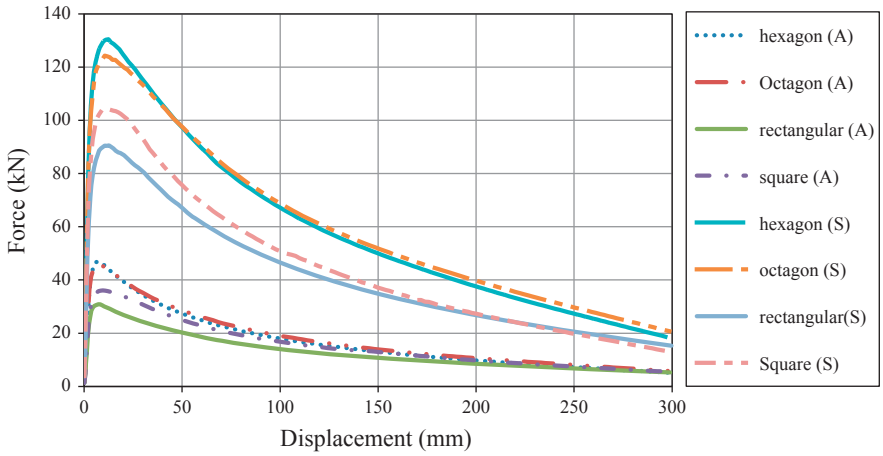

Fig. 5. Peak force vs. displacement for steel and aluminum with different cross-sections.

3.1. Influence of the cross-section of the S-shaped member

In this section, the effects from different cross-sectional (CS) shapes of the S-shaped members are addressed. Four different cross-sections were proposed, including square, rectangle, hexagon and octagon sections with perimeters of 534 mm and thicknesses of 3 mm. The impactor hits the S-shaped member with a high speed of 2000 mm/s and a ramping time of 0.05 s. Two different materials, steel and aluminum, are considered in this section. The specific energy absorption (SEA) is the main criterion used to assess the weight efficiency. The peak force is also used to define the optimum shape.

A summary of the results is presented in Table 1 and Figs. 4 and 5. The weight, SEA and peak force for different cross-sections for both steel and aluminum materials are clearly presented. It is shown for both materials that the S-shaped member with the hexagonal cross-section produces the best values of the specific energy absorption (SEA). Although aluminum has a 17% lower SEA value than steel, it produces a 65% savings in the total weight, which is considered to be a large benefit compared to the SEA criterion. In all models, the force increases up to the peak value and then decays dramatically. In addition, the peak force in the aluminum case is reduced by 65% compared to the steel material.

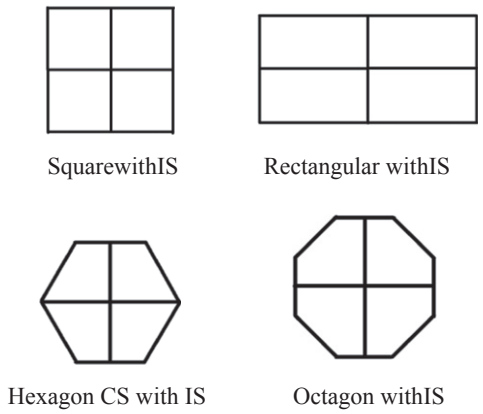

Fig. 6. Different cross-sections of an S-shaped member with inner stiffeners (Type 1).

3.2. Influence of inner stiffeners for different cross-sections of the S-shaped members

The influence of adding Type 1 inner stiffeners (IS) to S-shaped members is presented in this section and is shown in Fig. 6. The thickness of the inner stiffeners is taken as 3 mm, and they are made of the same materials as the S-shaped members.

The summary of the results are presented in Table 2 and Figs. 7 and 8. The weight, SEA and peak force for different cross-sections for both steel and aluminum materials are clearly presented. It is shown for both materials that the S-shaped member with an octagonal cross-section produces the best values of the specific energy absorption (SEA). The aluminum has 14.8% lower SEA values than steel, but it produces a 65% savings in the total weight, which is considered to be a large benefit compared to the SEA reduction. In addition, the peak force in the aluminum cases were reduced by 64% compared to the steel material. It is also noted that adding inner stiffeners enhanced the SEA, but the weight and peak force are increased. For octagonal aluminum, the SEA is enhanced by 22.5% but the weight and peak force are increased by 60% and 65%, respectively. Similarly, the SEA in steel samples is enhanced by 23%, but the weight and peak force are increased by 60% and 66%, respectively.

It is worth noting that the hexagonal cross-section presents better results without the inner stiffeners. However, the addition of inner stiffeners makes the octagon shapes the most optimal cross-section overall.

Table 2
SEA and peak force of steel and aluminum S-shaped longitudinal members with different cross-sections having inner stiffeners.

	Aluminum			Steel		
	Weight (kg)	SEA (kJ/kg)	Peak force (kN)	Weight (kg)	SEA (kJ/kg)	Peak force (kN)
Hexagon with IS	7.641	0.999	72.951	22.160	1.192	204.549
Octagon with IS	7.553	1.122	75.863	21.903	1.317	206.826
Rectangle with IS	7.209	0.899	56.968	20.906	1.046	162.013
Square with IS	7.073	1.006	65.177	20.511	1.135	181.596

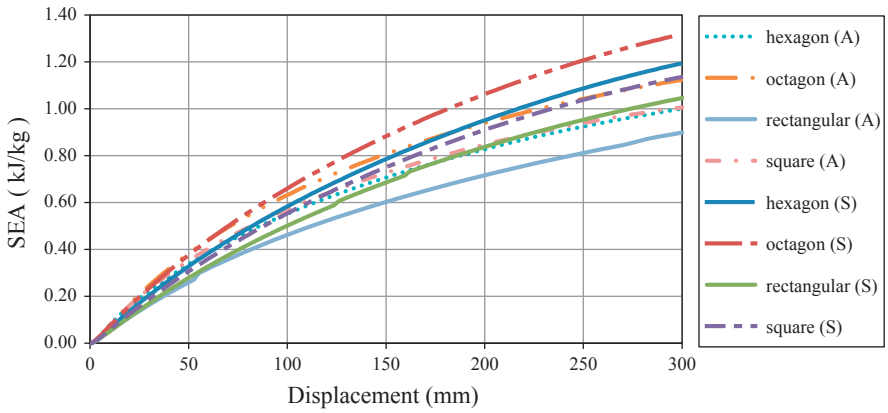

Fig. 7. SEA vs. displacement for steel and aluminum with different cross-sections having inner stiffeners.

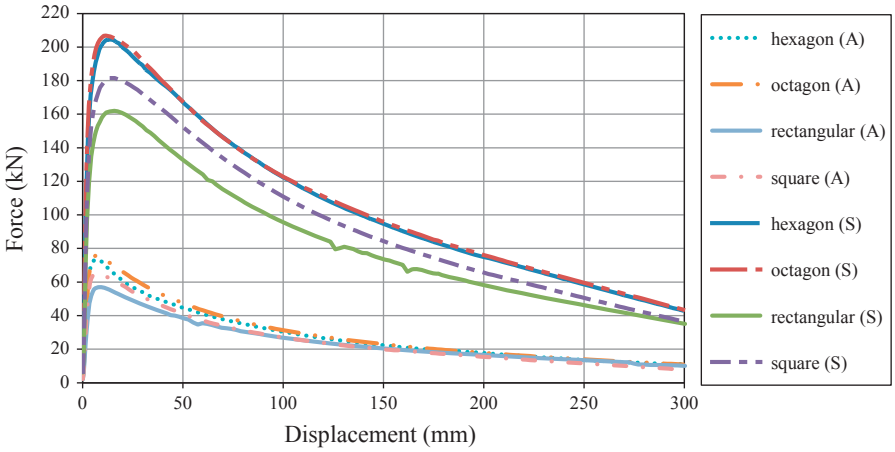

Fig. 8. Peak force vs. displacement for steel and aluminum with different cross-sections having inner stiffeners.

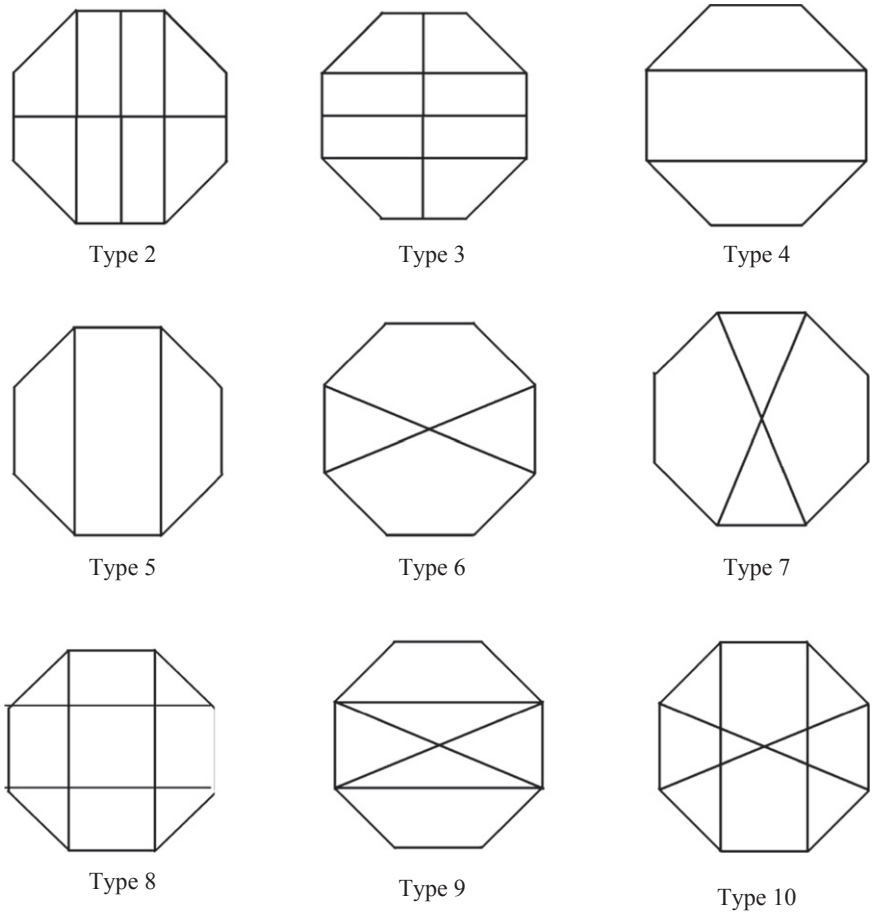

Fig. 9. Different inner stiffening members for the octagon cross-sections of the S-shaped member.

Table 3
SEA and peak force of steel and aluminum S-shaped longitudinal members with octagonal cross-sections having different types of inner stiffeners.

	Aluminum			Steel		
	Weight (kg)	SEA (kJ/kg)	Peak force (kN)	Weight (kg)	SEA (kJ/kg)	Peak force (kN)
Type 1	7.553	1.122	75.863	21.903	1.317	206.826
Type 2	10.377	1.167	102.522	30.093	1.377	291.236
Type 3	10.420	1.153	102.582	30.218	1.342	290.480
Type 4	7.575	0.968	70.173	21.967	1.149	196.872
Type 5	7.531	1.006	71.565	21.841	1.234	199.913
Type 6	7.799	1.161	77.019	22.617	1.424	222.823
Type 7	7.765	1.222	78.629	22.520	1.549	226.610
Type 8	10.399	1.167	101.740	30.157	1.411	295.186
Type 9	10.666	1.034	93.882	30.933	1.248	273.731
Type 10	10.623	1.326	109.508	30.808	1.656	327.886

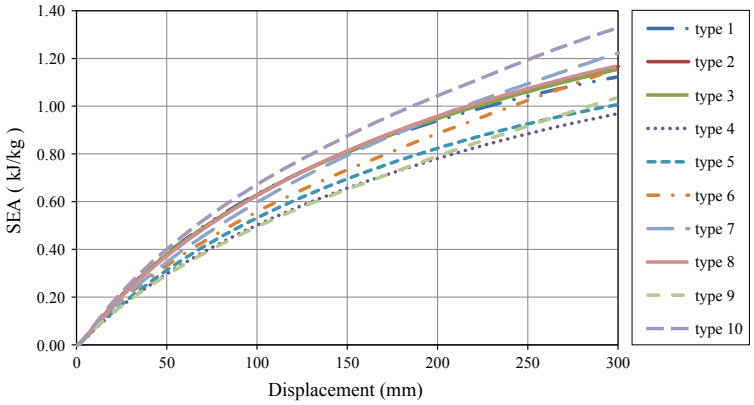

Fig. 10. SEA vs. displacement for aluminum members with octagonal cross-sections having different inner stiffeners.

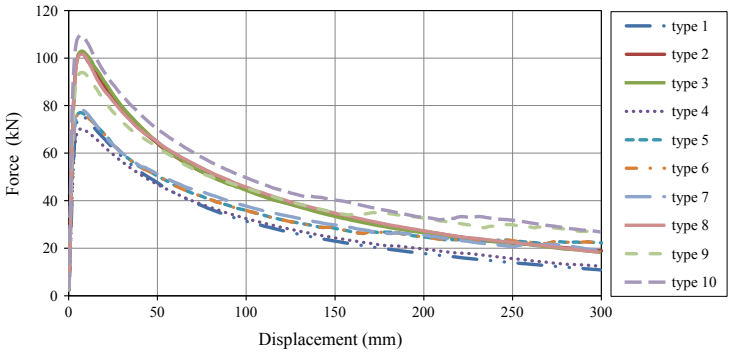

Fig. 11. Peak force vs. displacement for aluminum members with octagonal cross-sections having different inner stiffeners.

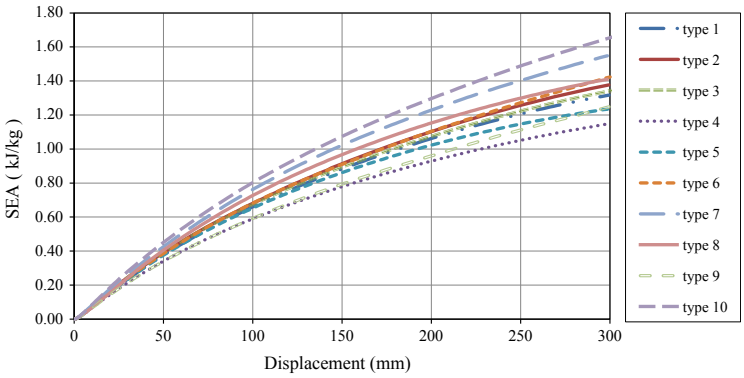

Fig. 12. SEA vs. displacement for steel members with octagonal cross-sections having different inner stiffeners.

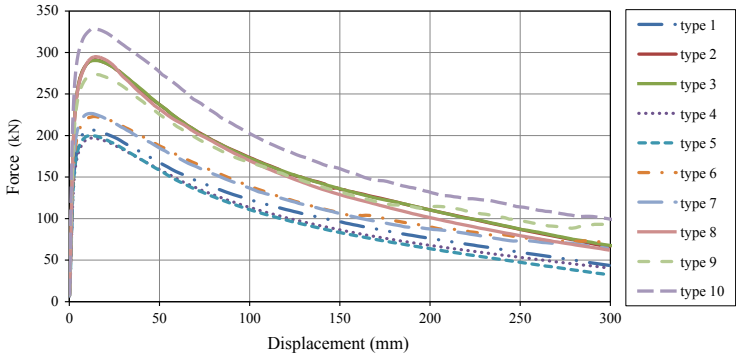

Fig. 13. Peak force vs. displacement for steel members with octagonal cross-sections having different inner stiffeners.

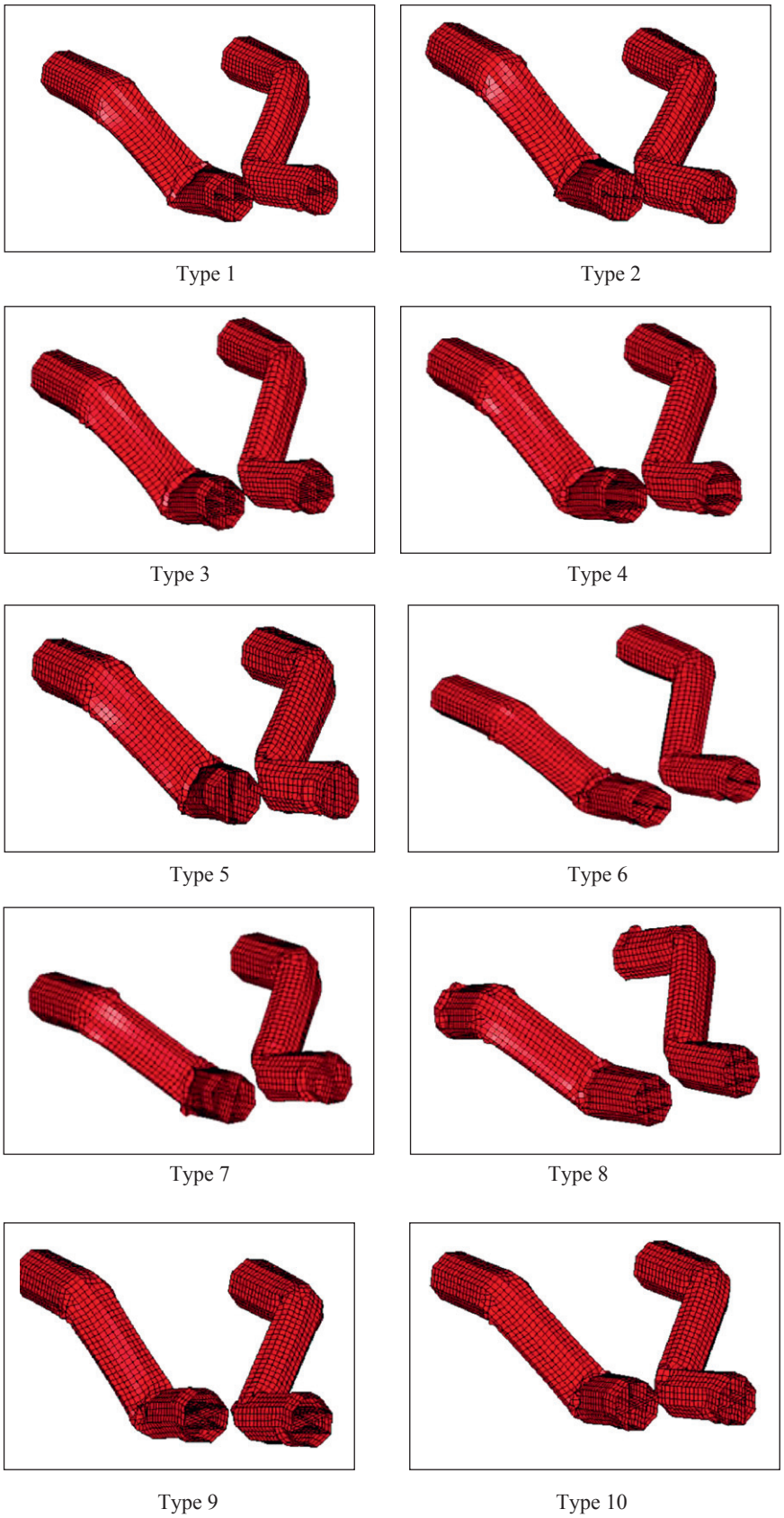

Fig. 14. Crashed steel octagonal S-shaped members for different types of inner stiffeners at time 0.1 s.

3.3. Influence of different inner stiffeners in S-shaped members with octagonal cross-section

Nine different combinations of inner stiffening members are used to modify and optimize the performance of the octagon S-shaped longitudinal member, as shown in Fig. 9. All of the inner stiffening types are made of the same material with thicknesses of 3 mm.

A summary of the results for the octagonal cross-section with different types of stiffeners for both steel and aluminum materials are clearly presented in Table 3. The SEA and peak force vs. displacement histories are depicted in Figs. 10 and 11 for aluminum and 12 and 13 for steel, respectively.

It is shown in both materials that the S-shaped member with Type 7 inner stiffeners produces the best values of specific energy absorption (SEA). The aluminum has a 21% lower SEA value compared to steel, but it produces a 65% savings in the total weight, which is considered to be a large benefit compared to the SEA criterion. In addition, the peak force in the aluminum case is reduced by 65.3% compared to the steel material. It is also noted

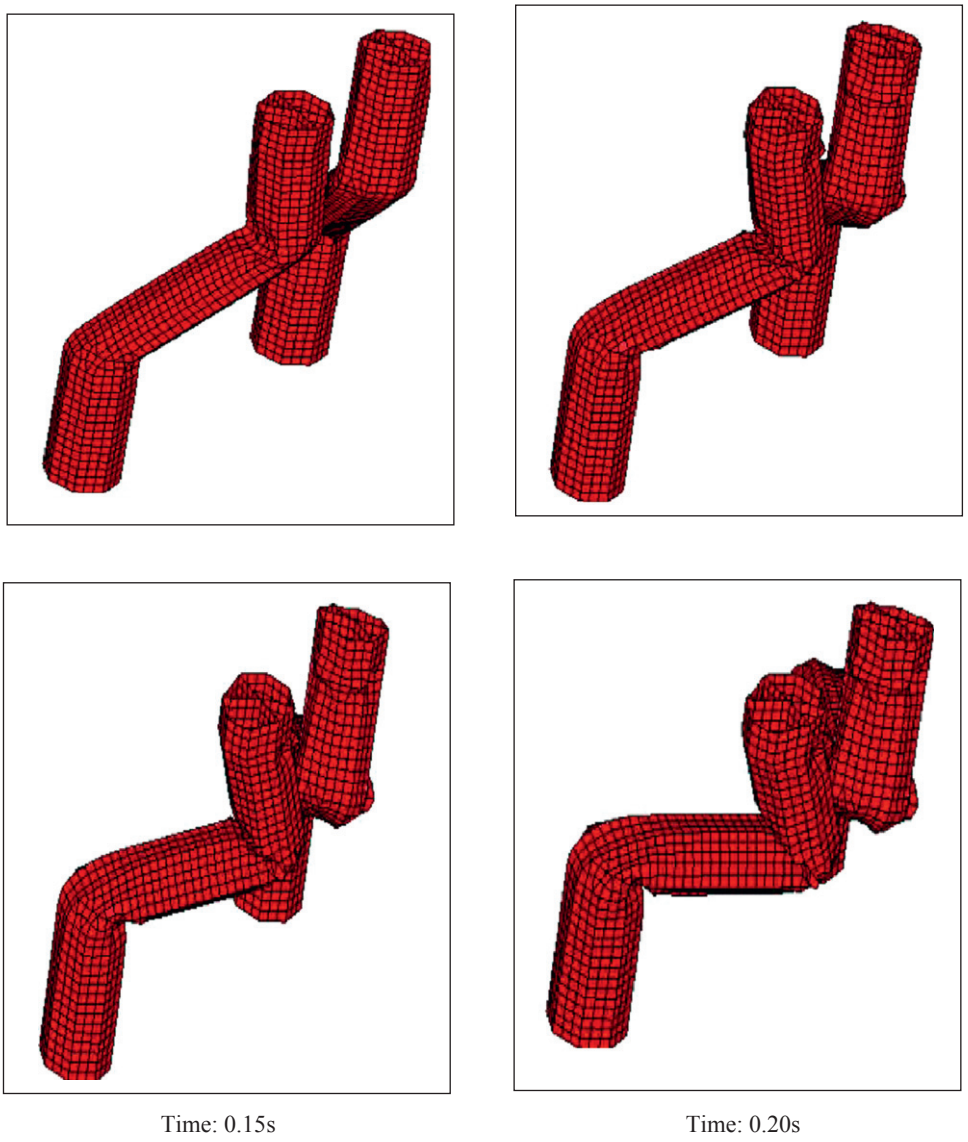

Fig. 15. Crashed steel Octagonal S-shaped members with Type 7 inner stiffeners at 0.05, 0.1, 0.15 and 0.20 s.

Table 4
SEA and peak force of steel and aluminum S-shaped longitudinal members with octagonal cross-sections having Type 7 inner stiffeners.

	Aluminum			Steel		
	Weight (kg)	SEA (kJ/kg)	Peak force (kN)	Weight (kg)	SEA (kJ/kg)	Peak force (kN)
$t=3$ mm	7.765	1.222	78.629	22.520	1.549	226.610
$t=6$ mm	15.531	1.615	185.030	45.040	1.890	551.223
$t=9$ mm	23.296	1.829	605.125	67.558	2.126	1832.680
$t=12$ mm	31.062	1.964	842.652	90.080	2.309	2586.770
$t=15$ mm	38.826	2.068	1085.370	112.599	2.582	3363.690

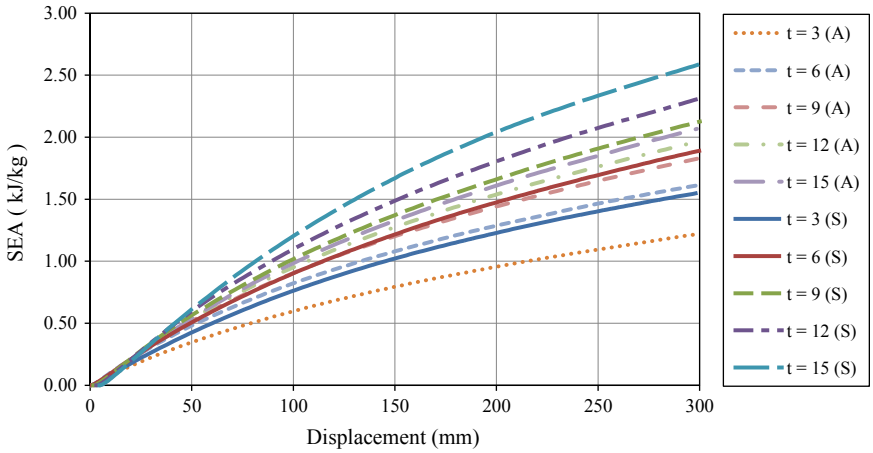

Fig. 16. SEA vs. displacement for aluminum and steel members with octagonal cross-sections having Type 7 inner stiffeners for different thicknesses of the S-shaped member.

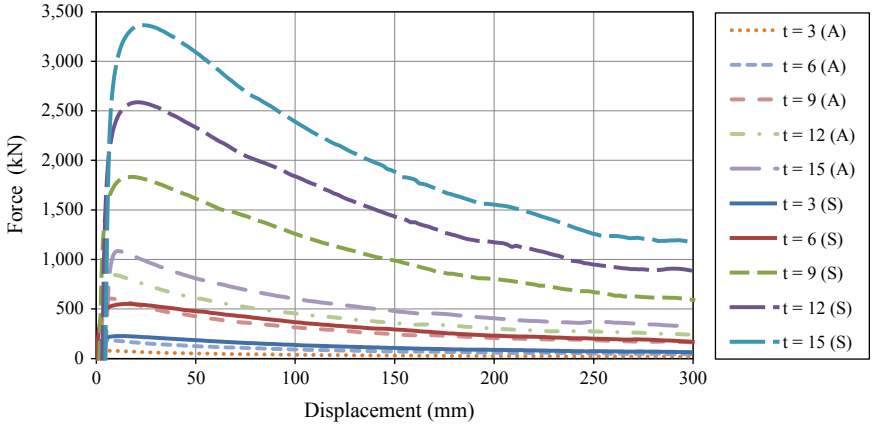

Fig. 17. Peak force vs. displacement for aluminum and steel members with octagonal cross-sections with Type 7 inner stiffeners for different thicknesses of the S-shaped member.

that adding the inner stiffeners (Type 10) enhances the SEA by 8% and 4.6% for aluminum and steel, respectively; however, the weight and the peak force are increased by 36.8% and 39% for aluminum and by 36.8% and 44.7% for steel, respectively.

The crashed steel octagonal S-shaped members for different types of inner stiffeners are shown in Figs. 12, 13 and 14 at time 0.1 s. Fig. 15 shows the crashed steel octagonal S-shaped members with Type 7 inner stiffeners at 0.05, 0.1, 0.15 and 0.20 s. The bending collapse dominates the response, and a single local axial fold is observed near the fixed, or impact, end. The bending resistance of aluminum members is low, which explains the small magnitude of the peak force.

3.4. Influence of different thicknesses for S-shaped members with octagonal cross-sections

In this section, the influence of different thicknesses on the octagonal cross-section with Type7 stiffeners is discussed. The different thicknesses of the thin-wall members used in the study are 6, 9, 12 and 15 mm.

A summary of the results for octagonal cross-section with Type 7 inner stiffeners for both steel and aluminum materials is clearly presented in Table 4. The SEA and peak force vs. displacement histories for different thicknesses of the S-shaped member are depicted in Figs. 16 and 17, respectively.

It is shown for both materials that the S-shaped member with a thickness of 3 mm produces the best results if the weight and peak force are considered. It is clearly shown that increasing the thickness will increase the SEA; however, the rate of SEA enhancement is very low compared to the huge increase in the weight and peak force. Using a 6-mm thickness will enhance the SEA for aluminum by 24%; however, it will cause a huge weight increase by doubling the weight of the member and increasing the peak force by 235%. Similarly, a 6-mm thickness in the steel member will double the weight and increase the peak force by 245%. In summary, increasing the thickness will enhance the SEA only very slightly when compared to the weight increase and the large added peak force. Therefore, the thickness of 3 mm was considered most suitable in this study.

4. Conclusions

This study was aimed at modifying the design of the frontal S-shaped longitudinal members to enhance the energy absorption ability and to minimize the peak force response. Several cross-sections with and without additional inner stiffening members were investigated in this study. In addition, the material type and the member thickness were also considered. The numerical simulations were carried out using the explicit finite element code LS-DYNA. From the results discussion presented in this paper for frontal impact of S-shaped longitudinal members, it is worth noting that the most desirable S-shaped member enhanced the specific energy absorption (SEA) while also reducing the

weight and peak force response during frontal impact. The results showed that an octagonal cross-section with Type 7 inner stiffeners (two vertical diagonal inner members) provide a good combination of structural reinforcements to increase the bending resistance of the members, and desirable results were produced including an SEA of 1.222 kJ/kg for aluminum and 1.59 kJ/kg for steel with peak forces of 78.629 kN and 226.610 kN, respectively.

References

[1] LS-DYNA, Livermore Software Technology Corporation. Livermore, California, USA; 2010.
[2] Ohkami Y, Takada K, Motomura K, Shimamura M, Tomizawa H, Usuda M. Collapse of thin-walled curved beam with closed-hat section—part 1: study on collapse characteristics. SAE Technical Paper 900460; 1990.
[3] Abe K, Nishigaki K, Ishivama S, Ohta M, Takagi M, Matsukawa F, et al. Collapse of thin-walled curved beam with closed-hat section—part 2: Simulation by plane plastic hinge model,'' SAE Technical Paper 900461; 1990.
[4] Kim H, Wierzbicki T. Effect of the cross-sectional shape of hat-type cross-sections on crash resistance of an "S"-frame. Thin-Walled Structures 2001;39:535–54.
[5] Zhang C, Saigal A. Crash behavior of a 3D S-shape space frame structure. Journal of Materials Processing Technology 2007;191:256–9.
[6] Hosseini-Tehrani P, Nikahd M. Effects of ribs on S-frame crashworthiness. Proceeding of IMechE Part D: Journal of Automobile Engineering 2006;220: 1679–89.
[7] Hosseini-Tehrani P, Nikahd M. Two materials S-frame representation for improving crashworthiness and lightening. Thin-Walled Structures 2006;44: 407–14.
[8] Oliveira D, Worswick M, Grantab R, Williams B, Mayer R. Effect of forming process variables on the crashworthiness of aluminum alloy tubes. International Journal of Impact Engineering. 2006;32:826–46.
[9] Kim H, Chen W, Wierzbicki T. Weight and crash optimization of foam-filled three-dimensional S frame. Computational Mechanics 2002;28:417–24.
[10] Mamalis A, Manolakos D, Ioannidis M, Papapostolou D. Crashworthy characteristics of axially statically compressed thin-walled square CFRP composite tubes: experimental. Composite Structures 2004;63:347–60.
[11] Elmarakbi A, Fielding N, Hadavinia H. Finite element simulation of the axial crush of thin-walled tubes with different cross-sections: vehicle/pole impact application. International Journal of Vehicle Structures and Systems[Special Issue on Impact and Crashworthiness of Metals Structures] 2011;3:154–60.
[12] ASTM International. Metals Handbook. Vol. 2—properties and selection: nonferrous alloys and special purpose materials. 10th ed1990.